Chapter 6. Time and Frequency Characterization of Signal and Systems

§6.1 The Magnitude-Phase Representation of The Fourier Transform

$$\begin{cases} X(j\omega) = |X(j\omega)|\, e^{j\measuredangle X(j\omega)} \\ X(e^{j\omega}) = |X(e^{j\omega})|\, e^{j\measuredangle X(e^{j\omega})} \end{cases}$$

In general, changes in both the phase function and the magnitude function lead to changes in the time-domain characteristics of the signal $x(t)$.

- The auditory systems are insensitive to phase
- Tape Recording signal $x(t) \in R$:

$$\mathcal{F}\{x(-t)\} = X(-j\omega) = |X(j\omega)|\, e^{-j\measuredangle X(j\omega)}$$

played backward.

- In pictures, the phase captures the information about the edges

  See Fig 6.2 (2-D Fourier Series on the backside)

§6.2 The Magnitude-Phase Representation of The Frequency Response of LTI systems

$$Y(j\omega) = H(j\omega)X(j\omega) \Rightarrow \begin{cases} |Y(j\omega)| = |H(j\omega)|\,|X(j\omega)| \\ \measuredangle Y(j\omega) = \measuredangle H(j\omega) + \measuredangle X(j\omega) \end{cases}$$

$$Y(e^{j\omega}) = H(e^{j\omega})X(e^{j\omega}) \Rightarrow \begin{cases} |Y(e^{j\omega})| = |H(e^{j\omega})|\,|X(e^{j\omega})| \\ \measuredangle Y(e^{j\omega}) = \measuredangle H(e^{j\omega}) + \measuredangle X(e^{j\omega}) \end{cases}$$

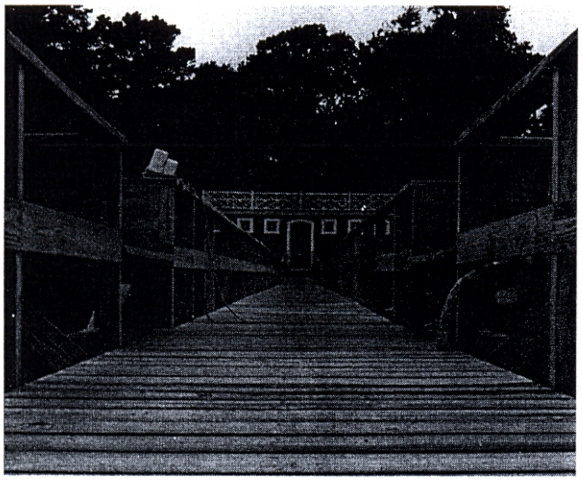

(a)

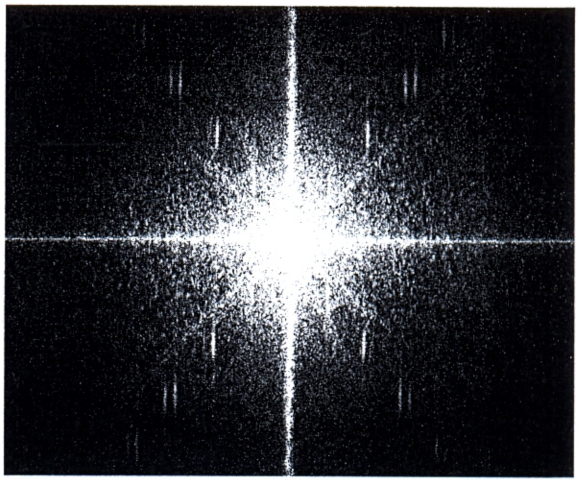

(b)

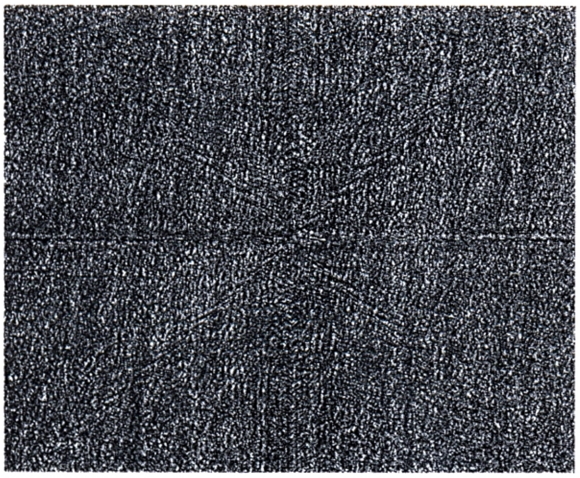

(c)

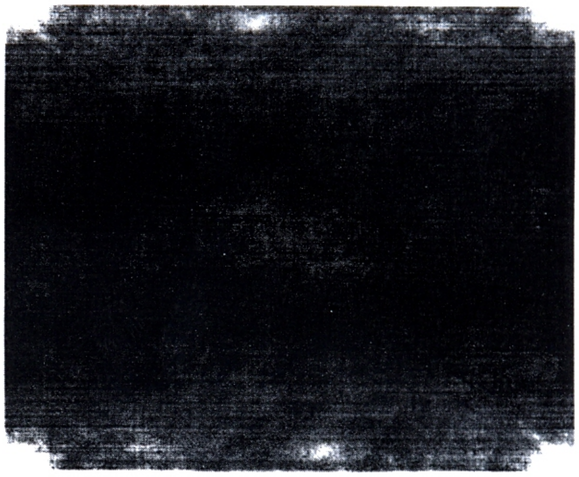

(d)

intensity in a picture are places at which complex exponentials at different frequencies are in phase. Therefore, it seems plausible to expect the phase of the Fourier transform of a picture to contain much of the information in the picture, and in particular, the phase should capture the information about the edges. To substantiate this expectation, in Figure 6.2(a) we have repeated the picture shown in Figure 1.4. In Figure 6.2(b) we have depicted the magnitude of the two-dimensional Fourier transform of the image in Figure 6.2(a), where in this image the horizontal axis is ω_1, the vertical is ω_2, and the brightness of the image at the point (ω_1, ω_2) is proportional to the magnitude of the transform $X(j\omega_1, j\omega_2)$ of the image in Figure 6.2(a). Similarly, the phase of this transform is depicted in Figure 6.2(c). Figure 6.2(d) is the result of setting the phase [Figure 6.2(c)] of $X(j\omega_1, j\omega_2)$ to zero (without changing its magnitude) and inverse transforming. In Figure 6.2(e) the magnitude of $X(j\omega_1, j\omega_2)$ was set equal to 1, but the phase was kept unchanged from what it was in Figure 6.2(c). Finally, in Figure 6.2(f) we have depicted the image obtained by inverse transforming the function obtained by using the phase in Figure 6.2(c) and the magnitude of the transform of a *completely different* image—the picture shown in Figure 6.2(g)! These figures clearly illustrate the importance of phase in representing images.

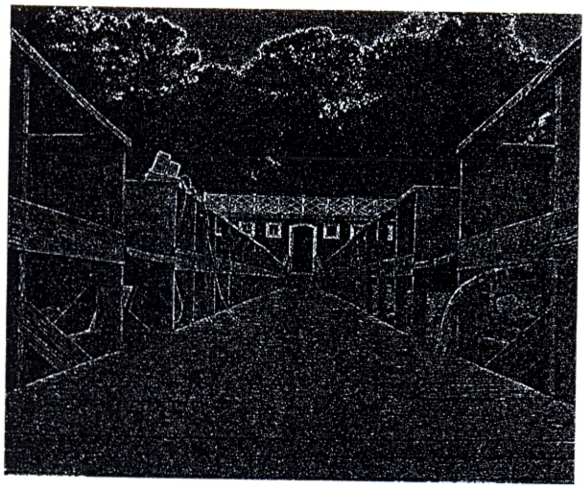

(e)

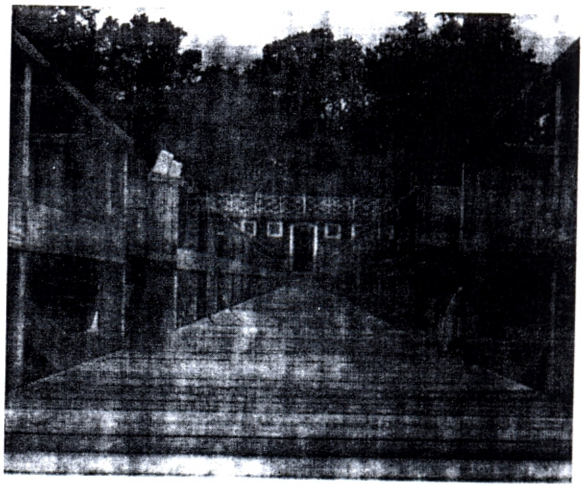

(f)

(g)

Figure 6.2 (a) The image shown in Figure 1.4; (b) magnitude of the two-dimensional Fourier transform of (a); (c) phase of the Fourier transform of (a); (d) picture whose Fourier transform has magnitude as in (b) and phase equal to zero; (e) picture whose Fourier transform has magnitude equal to 1 and phase as in (c); (f) picture whose Fourier transform has phase as in (c) and magnitude equal to that of the transform of the picture shown in (g).

6.2 THE MAGNITUDE-PHASE REPRESENTATION OF THE FREQUENCY RESPONSE OF LTI SYSTEMS

From the convolution property for continuous-time Fourier transforms, the transform $Y(j\omega)$ of the output of an LTI system is related to the transform $X(j\omega)$ of the input to the system by the equation

$$Y(j\omega) = H(j\omega)X(j\omega),$$

where $H(j\omega)$ is the frequency response of the system—i.e., the Fourier transform of the system's impulse response. Similarly, in discrete time, the Fourier transforms of the input $X(e^{j\omega})$ and ouput $Y(e^{j\omega})$ of an LTI system with frequency response $H(e^{j\omega})$ are related by

$$Y(e^{j\omega}) = H(e^{j\omega})X(e^{j\omega}). \tag{6.4}$$

Thus, the effect that an LTI system has on the input is to change the complex amplitude of each of the frequency components of the signal. By looking at this effect in terms of the magnitude-phase representation, we can understand the nature of the effect in more

$$\Rightarrow \begin{cases} |H(j\omega)|,\ |H(e^{j\omega})| & : \text{gain} \\ \angle H(j\omega),\ \angle H(e^{j\omega}) & : \text{phase shift} \end{cases}$$

$$\begin{cases} \angle H(j\omega) > 0 & : \text{phase lead} \\ \angle H(j\omega) < 0 & : \text{phase lag} \end{cases}$$

If the input is changed in a unwanted manner, the effects in gain and phase shift are commonly refered to as magnitude and phase distortion.

§6.2.1 Linear and Nonlinear phase

$$H(j\omega) = e^{-j\omega t_0} \Rightarrow \begin{cases} |H(j\omega)| = 1 \\ \angle H(j\omega) = -\omega t_0 & : \text{linear phase} \end{cases}$$

$$\Rightarrow y(t) = x(t-t_0) \ : \text{no distortion}$$

$|H(j\omega)| = 1$: all-pass system

§6.2.2 Group Delay

$$\tau(\omega) \triangleq -\frac{d}{d\omega} \angle H(j\omega) \qquad (6.14)$$

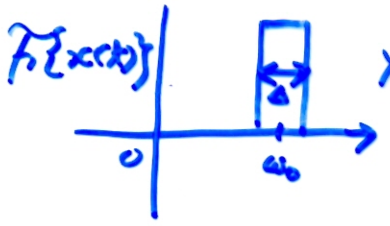

$\Delta \ll 1$

$$X(j\omega) \longrightarrow \boxed{H(j\omega)} \longrightarrow Y(j\omega)$$

$$Y(j\omega) \simeq X(j\omega)\,|H(j\omega_0)|\, e^{-j\{\tau(\omega_0)\omega + \phi\}}$$

$$\Rightarrow y(t) \simeq |H(j\omega_0)|\, e^{-j\phi}\, x(t - \tau(\omega_0))$$

where $\angle H(j\omega_0) + \tau(\omega_0)\omega = -\phi$

6-3

$$\langle \text{Example } 6.1 \rangle \quad H(j\omega) \triangleq \prod_{i=1}^{3} H_i(j\omega) \triangleq \prod_{i=1}^{3} \frac{(1+(j\omega/\omega_i)^2 - 2j\zeta_i(\omega/\omega_i)}{(1+(j\omega/\omega_i)) + 2j\zeta_i(\omega/\omega_i)}$$

$$\begin{cases} \zeta_1 = 0.066, & \zeta_2 = 0.033, & \zeta_3 = 0.058 \\ f_1 = 50\,Hz, & f_2 = 150\,Hz, & f_3 = 300\,Hz \end{cases}$$

$|H_i(j\omega)| = 1, \; i = 1, 2, 3$

$$\measuredangle H_i(j\omega) = -2\tan^{-1}\left[\frac{2\zeta_i\,\omega/\omega_i}{1+(\omega/\omega_i)^2}\right]$$

$2\pi k$

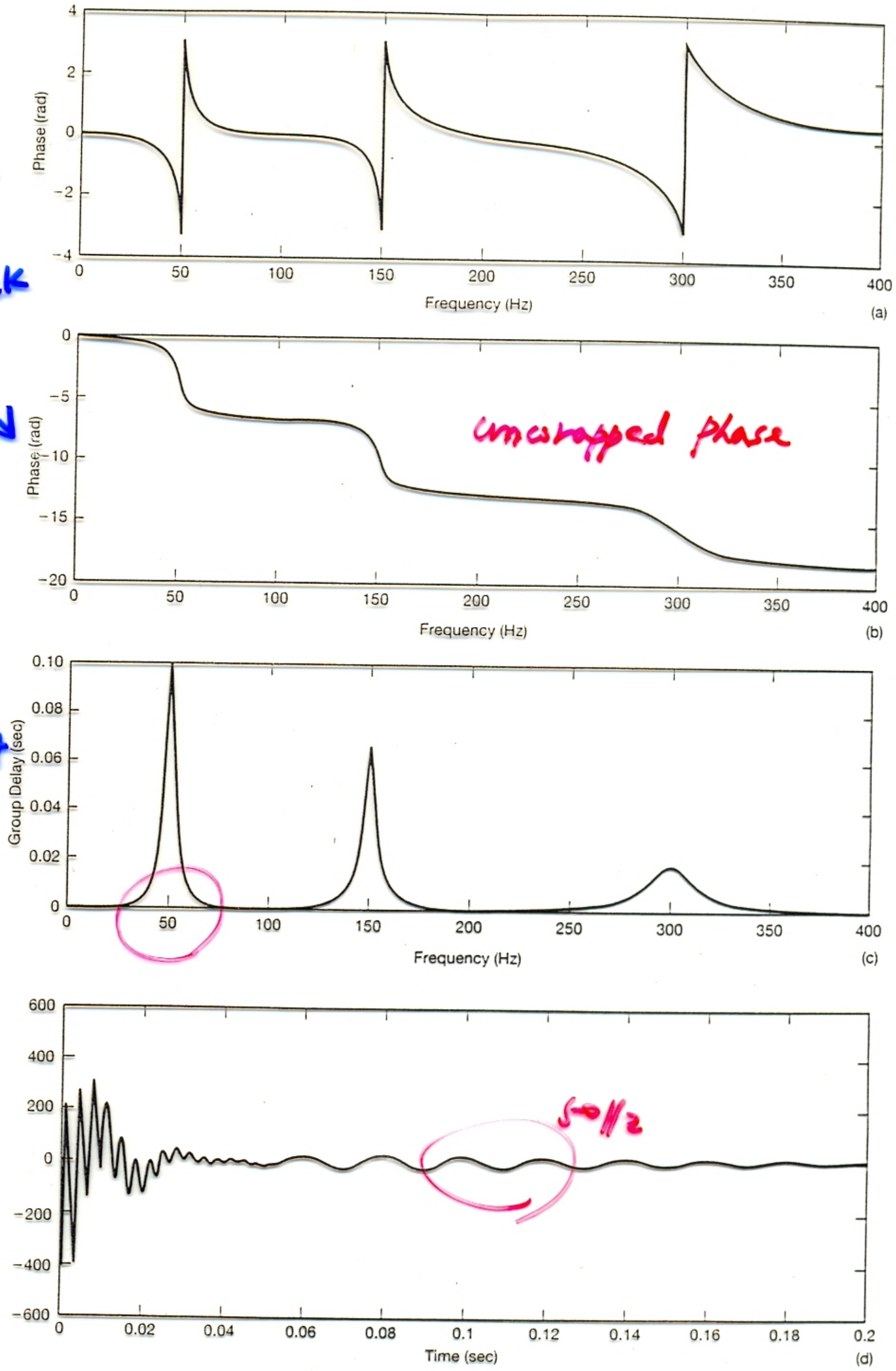

Different frequencies in the input are delayed by different amounts : dispersion

Figure 6.5 Phase, group delay, and impulse response for the all-pass system of Example : (a) principal phase; (b) unwrapped phase; (c) group delay; (d) impulse response. Each of these quantities is plotted versus frequency measured in Hertz.

§ 6.2.3 Log-Magnitude and Bode Plots

- $20 \log_{10}$: decibel (dB)
- The use of a logarithmic frequency scale

① a much wider range of frequencies to be displayed

② the shape is invariant under frequency scaling

③ an approximate sketch is easily obtained through the use of asymptotes

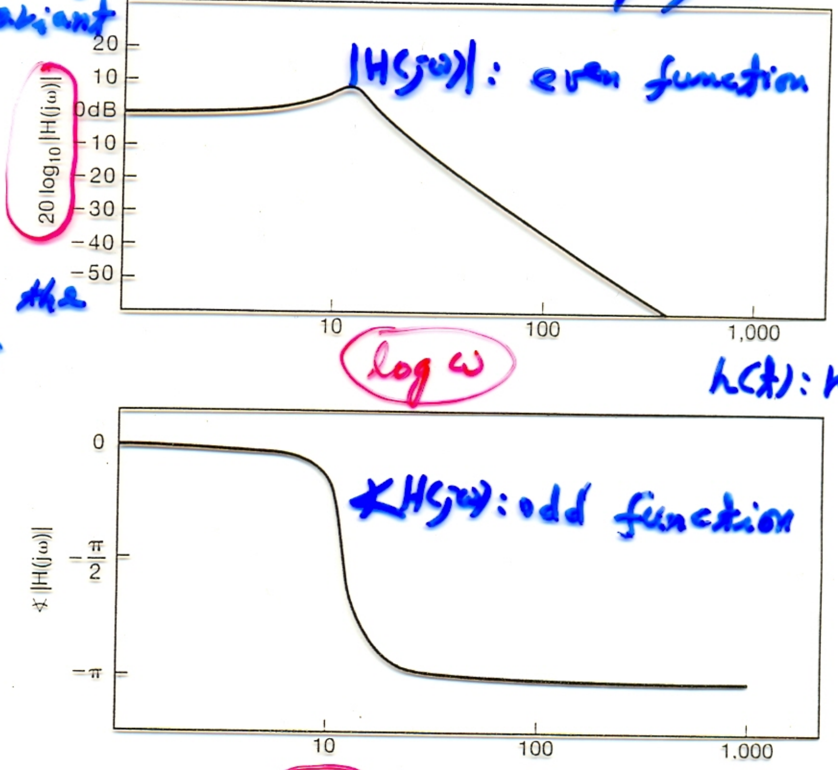

Figure 6.8 A typical Bode plot. (Note that ω is plotted using a logarithmic scale.)

of a particular response curve doesn't change if the frequency is scaled. (See Problem 6.30.) Furthermore for continuous-time LTI systems described by differential equations, an approximate sketch of the log magnitude vs. log frequency can often be easily obtained through the use of asymptotes. In Section 6.5, we will illustrate this by developing simple piecewise-linear approximate Bode plots for first- and second-order continuous-time systems.

In discrete time, the magnitudes of Fourier transforms and frequency responses are often displayed in dB for the same reasons that they are in continuous time. However, in discrete time a logarithmic frequency scale is not typically used, since the range of frequencies to be considered is always limited and the advantage found for differential equations (i.e., linear asymptotes) does not apply to difference equations. Typical graphical representations of the magnitude and phase of a discrete-time frequency response are shown in Figure 6.9. Here, we have plotted $\sphericalangle H(e^{j\omega})$ in radians and $|H(e^{j\omega})|$ in decibels [i.e., $20 \log_{10} |H(e^{j\omega})|$] as functions of ω. Note that for $h[n]$ real, we actually need plot $H(e^{j\omega})$ only for $0 \le \omega \le \pi$, because in this case the symmetry property of the Fourier transform implies that we can then calculate $H(e^{j\omega})$ for $-\pi \le \omega \le 0$ using the relations $|H(e^{j\omega})| = |H(e^{-j\omega})|$ and $\sphericalangle H(e^{-j\omega}) = -\sphericalangle H(e^{j\omega})$. Furthermore, we need not consider values of $|\omega|$ greater than π, because of the periodicity of $H(e^{j\omega})$.

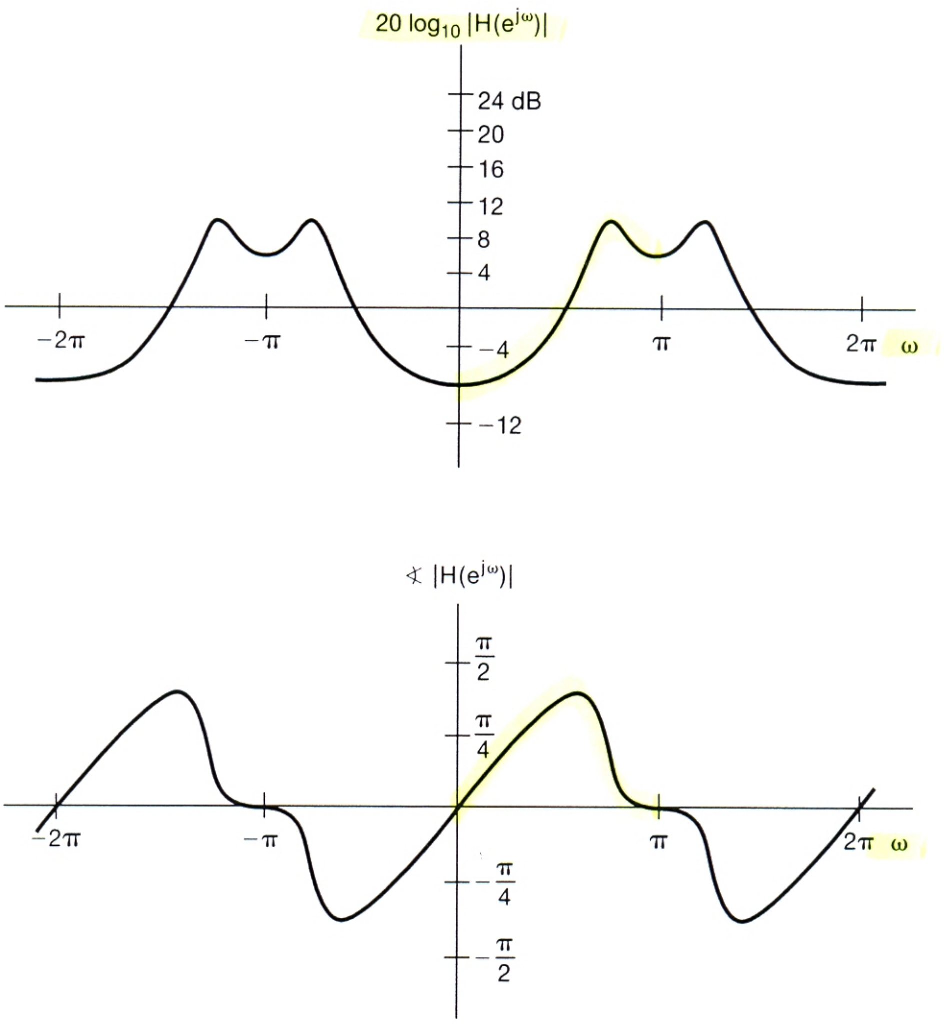

Figure 6.9 Typical graphical representations of the magnitude and phase of a discrete-time frequency response $H(e^{j\omega})$.

As emphasized in this section, a logarithmic amplitude scale is often useful and important. However, there are many situations in which it is convenient to use a linear amplitude scale. For example, in discussing ideal filters for which the magnitude of the frequency response is a nonzero constant over some frequency bands and zero over others, a linear amplitude scale is more appropriate. Thus, we have introduced both linear and logarithmic graphical representations for the magnitude of the Fourier transform and will use each as appropriate.

6.3 TIME-DOMAIN PROPERTIES OF IDEAL FREQUENCY-SELECTIVE FILTERS

In Chapter 3, we introduced the class of frequency-selective filters, i.e., LTI systems with frequency responses chosen so as to pass one or several bands of frequencies with little or no attenuation and to stop or significantly attenuate frequencies outside those bands. As we discussed in Chapters 3, 4, and 5, there are a number of issues of importance that arise

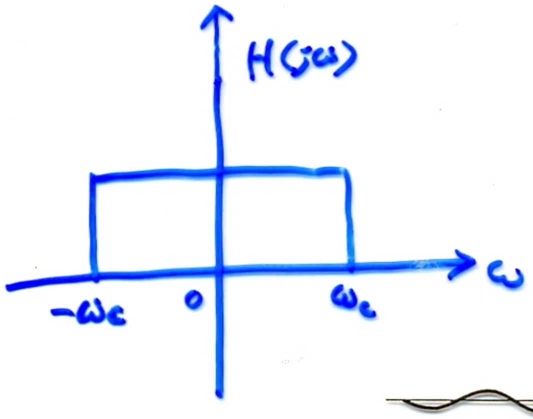

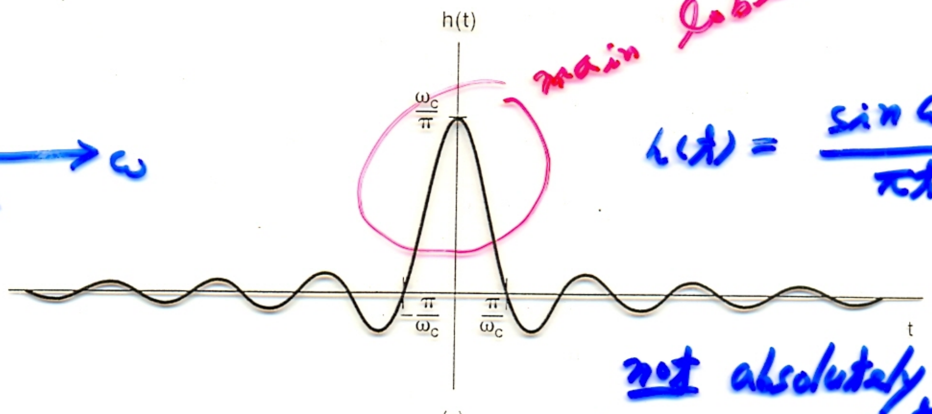

main lobe

$h(t) = \dfrac{\sin \omega_c t}{\pi t}$

not absolutely integrable

(a)

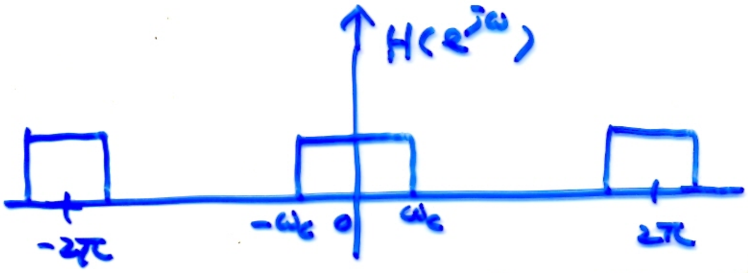

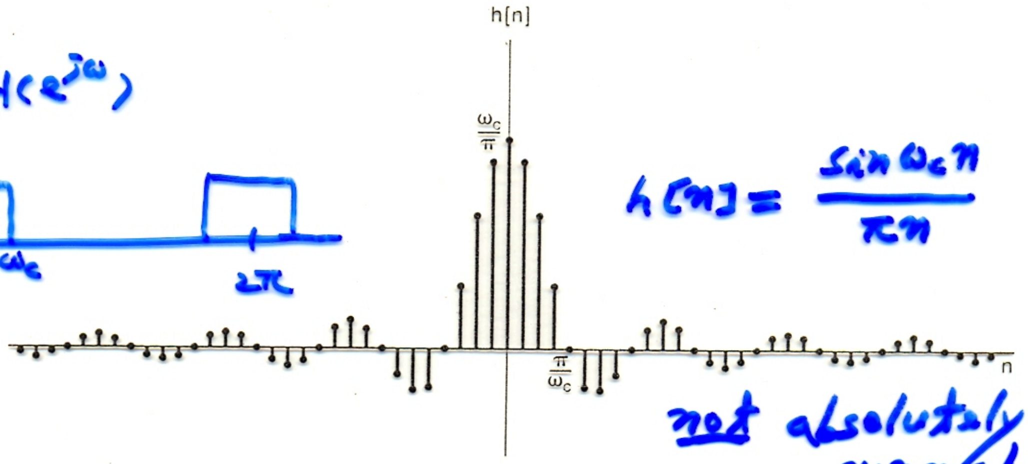

$h[n] = \dfrac{\sin \omega_c n}{\pi n}$

not absolutely summable

(b)

Figure 6.12 (a) The impulse response of the continuous-time ideal lowpass filter of Figure 6.10(a); (b) the impulse response of the discrete-time ideal lowpass filter of Figure 6.10(b) with $\omega_c = \pi/4$.

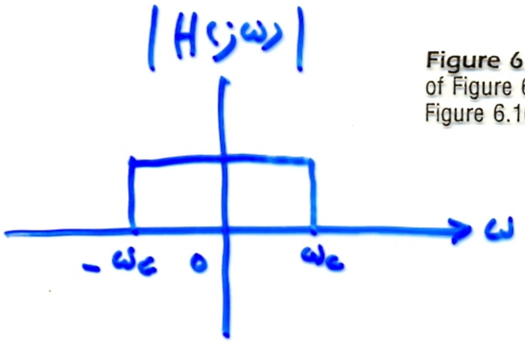

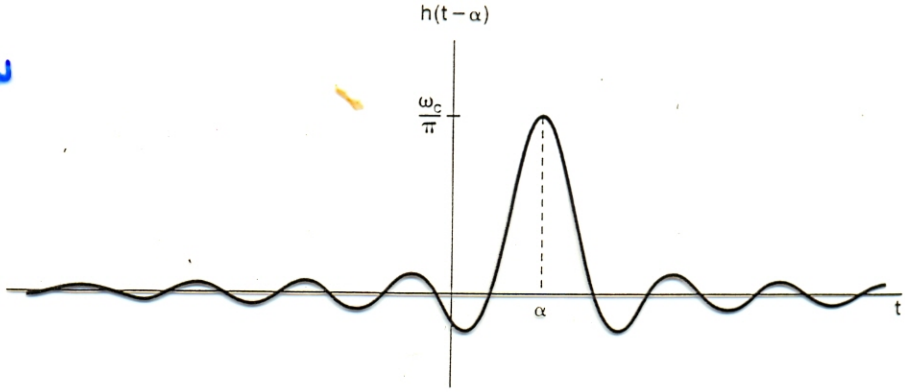

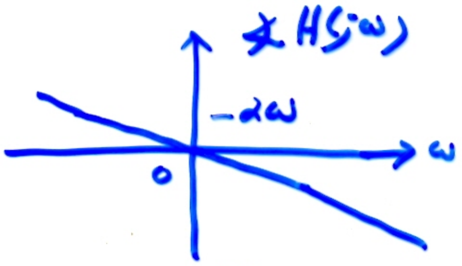

Figure 6.13 Impulse response of an ideal lowpass filter with magnitude and phase shown in Figure 6.11.

The step responses $s(t)$ and $s[n]$ of the ideal lowpass filters in continuous time and discrete time are displayed in Figure 6.14. In both cases, we note that the step responses exhibit several characteristics that may not be desirable. In particular, for these filters, the step responses overshoot their long-term final values and exhibit oscillatory behavior, frequently referred to as *ringing*. Also, recall that the step response is the running integral or sum of the impulse response—i.e.,

$$s(t) = \int_{-\infty}^{t} h(\tau)d\tau,$$

$$s[n] = \sum_{m=-\infty}^{n} h[m].$$

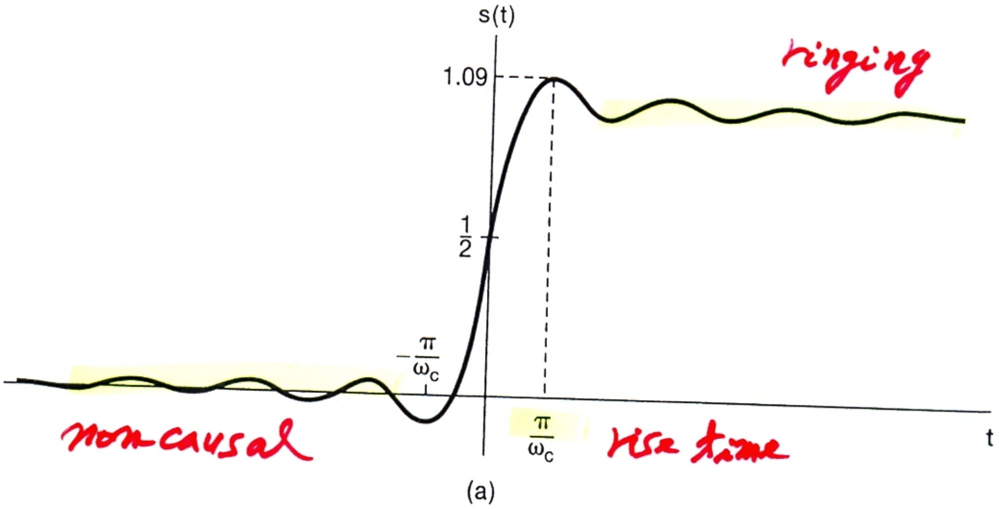

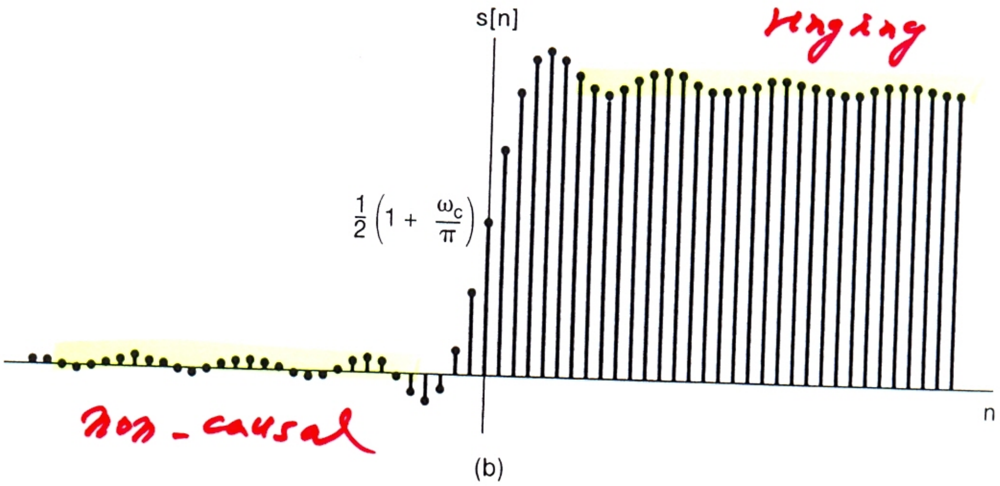

Figure 6.14 (a) Step response of a continuous-time ideal lowpass filter; (b) step response of a discrete-time ideal lowpass filter.

6-8

Since the impulse responses for the ideal filters have main lobes extending from $-\pi/\omega_c$ to $+\pi/\omega_c$, the step responses undergo their most significant change in value over this time interval. That is, the so-called *rise time* of the step response, a rough measure of the response time of the filter, is also inversely related to the bandwidth of the filter.

6.4 TIME-DOMAIN AND FREQUENCY-DOMAIN ASPECTS OF NONIDEAL FILTERS

1 The characteristics of ideal filters are not always desirable in practice. For example, in many filtering contexts, the signals to be separated do not always lie in totally disjoint frequency bands. A typical situation might be that depicted in Figure 6.15, where the spectra of two signals overlap slightly. In such a case, we may wish to trade off the fidelity with which the filter preserves one of these signals—say, $x_1(t)$—against the level to which frequency components of the second signal $x_2(t)$ are attenuated. A filter with a gradual transition from passband to stopband is generally preferable when filtering the superposition of signals with overlapping spectra.

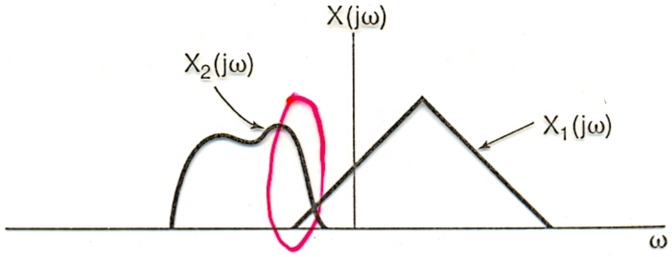

Figure 6.15 Two spectra that are slightly overlapping.

2 Another consideration is suggested by examining the step responses of ideal lowpass filters, shown in Figure 6.14. For both continuous time and discrete time, the step response asymptotically approaches a constant equal to the value of the step. In the vicinity of the discontinuity, however, it overshoots this value and exhibits ringing. In some situations, this time-domain behavior may be undesirable.

3 Moreover, even in cases where the ideal frequency-selective characteristics are desirable, they may not be attainable. For example, from eqs. (6.18) and (6.19) and Figure 6.12, it is evident that the ideal lowpass filter is noncausal. When filtering is to be carried out in real time, however, causality is a necessary constraint, and thus, a causal approximation to the ideal characteristics would be required. A further consideration that motivates providing some flexibility in the filter characteristics is ease of implementation. In general, the more precisely we try to approximate or implement an ideal frequency-selective filter, the more complicated or costly the implementation becomes, whether in terms of components such as resistors, capacitors, and operational amplifiers in continuous time or in terms of memory registers, multipliers, and adders in discrete time. In many contexts, a precise filter characteristic may not be essential and a simple filter will suffice.

For all of these reasons, nonideal filters are of considerable practical importance, and the characteristics of such filters are frequently specified or quantified in terms of several parameters in both the frequency and time domain. First, because the magnitude characteristics of the ideal frequency-selective filter may be unachievable or undesirable, it is preferable to allow some flexibility in the behavior of the filter in the passband and in the stopband, as well as to permit a more gradual transition between the passband and stopband, as opposed to the abrupt transition characteristic of ideal filters. For example, in the case of lowpass filters, the specifications may allow some deviation from unity gain in the passband and from zero gain in the stopband, as well as including both a passband edge and stopband edge with a transition band between them. Thus, specifications for a continuous-time lowpass filter are often stated to require the magnitude of the frequency response of the filter to be restricted to the nonshaded area indicated in Figure 6.16. In this figure, a deviation from unity of plus and minus δ_1 is allowed in the passband, and a deviation of δ_2 from zero is allowed in the stopband. The amount by which the frequency response differs from unity in the passband is referred to as the *passband ripple*, and the amount by which it deviates from zero in the stopband is referred to as the *stopband ripple*. The frequency ω_p is referred to as the *passband edge* and ω_s as the *stopband edge*. The frequency range from ω_p to ω_s is provided for the transition from passband to stopband and is referred to as the *transition band*. Similar definitions apply to discrete-time lowpass filters, as well as to other continuous- and discrete-time frequency-selective filters.

Design Specification in freq. domain

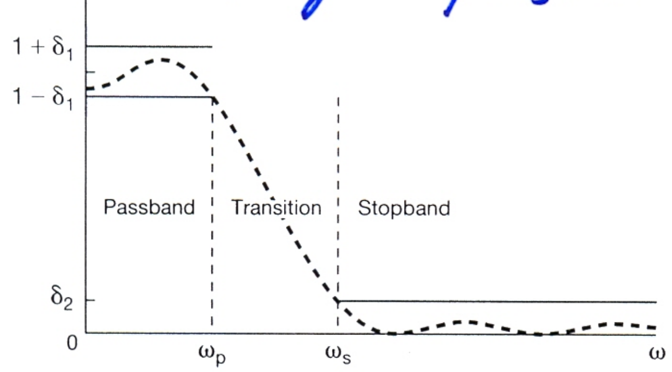

Figure 6.16 Tolerances for the magnitude characteristic of a lowpass filter. The allowable passband ripple is δ_1 and stopband ripple is δ_2. The dashed curve illustrates one possible frequency response that stays within the tolerable limits.

In addition to the specification of magnitude characteristics in the frequency domain, in some cases the specification of phase characteristics is also important. In particular, a linear or nearly linear phase characteristic over the passband of the filter is frequently desirable. for no distortion

To control the time-domain behavior, specifications are frequently imposed on the step response of a filter. As illustrated in Figure 6.17, one quantity often of interest is the rise time t_r of the step response—i.e., the interval over which the step response rises toward its final value. In addition, the presence or absence of oscillatory behavior, or ringing, in the step response is often of importance. If such ringing is present, then there are three other quantities that are often used to characterize the nature of these oscillations: the overshoot Δ of the final value of the step response, the ringing frequency ω_r, and the settling time t_s—i.e., the time required for the step response to settle to within a specified tolerance of its final value.

For nonideal lowpass filters, a trade-off may be observed between the width of the transition band (a frequency-domain characteristic) and the settling time of the step response (a time-domain characteristic). The following example illustrates this trade-off.

Design Spec. in Time Domain

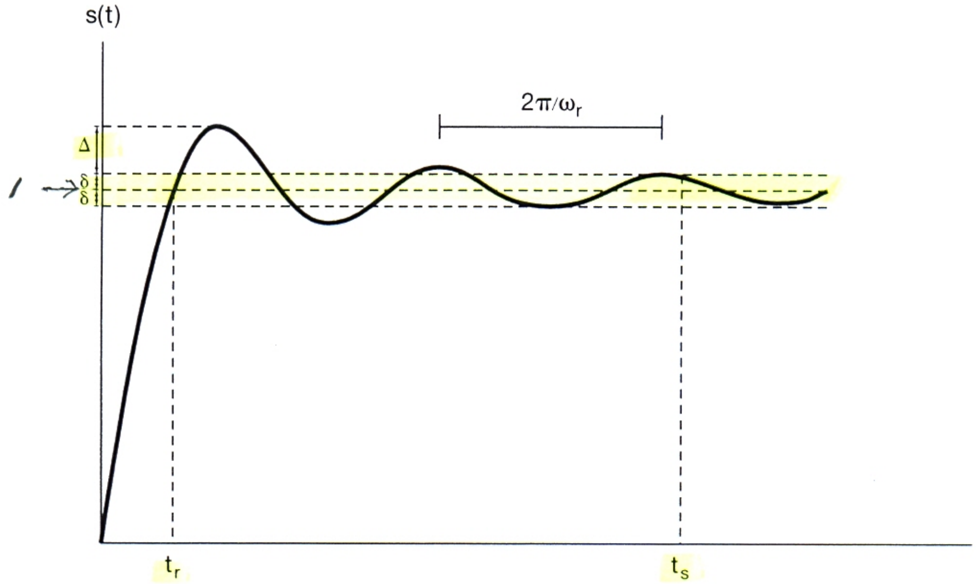

Figure 6.17 Step response of a continuous-time lowpass filter, indicating the rise time t_r, overshoot Δ, ringing frequency ω_r, and settling time t_s—i.e., the time at which the step response settles to within $\pm\delta$ of its final value.

Example 6.3

Let us consider two specific lowpass filters designed to have a cutoff frequency of 500 Hz. Each filter has a fifth-order rational frequency response and a real-valued impulse response. The two filters are of specific types, one referred to as Butterworth filters and the other as elliptic filters. Both of these classes of filters are frequently used in practice.

The magnitudes of the frequency responses of the two filters are plotted (versus frequency measured in Hertz) in Figure 6.18(a). We take the transition band of each filter as the region around the cutoff frequency (500 Hz) where the frequency response magnitude is neither within .05 of unity magnitude (the passband ripple) nor within .05 of zero magnitude (the stopband ripple). From Figure 6.18(a), it can be seen that the transition band of the Butterworth filter is *wider* than the transition band of the elliptic filter.

The price paid for the narrower transition band of the elliptic filter may be observed in Figure 6.18(b), in which the step responses of both filters are displayed. We see that the ringing in the elliptic filter's step response is more prominent than for the Butterworth step response. In particular, the settling time for the step response is longer in the case of the elliptic filter.

The consideration of the trade-offs between time-domain and frequency-domain characteristics and of other issues such as the complexity and cost of filters forms the core of the important field of filter design. In the next few sections, and in several of the problems at the end of the chapter, we provide additional examples of LTI systems and filters and their time- and frequency-domain characteristics.

6-10 <Example 6.3> $\delta_1 = \delta_2 = 0.5$, cutoff freq. 500 Hz
The transition band of the Butterworth filter is wider than that of the elliptic filter.

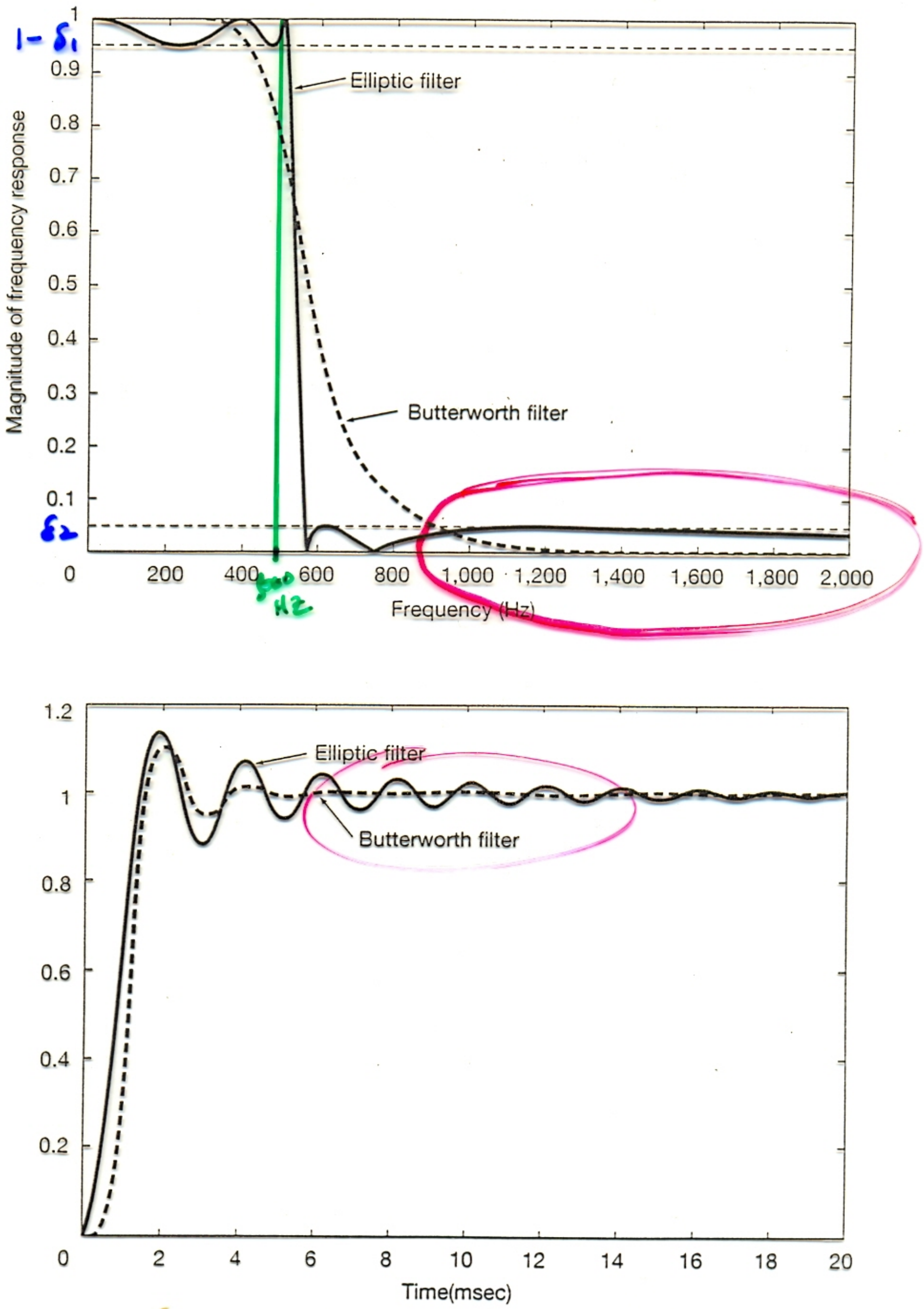

Figure 6.18 Example of a fifth-order Butterworth filter and a fifth-order elliptic filter designed to have the same passband and stopband ripple and the same cutoff frequency: (a) magnitudes of the frequency responses plotted versus frequency measured in Hertz; (b) step responses.

<u>Remark</u>

The consideration of the trade-offs between time-domain and frequency-domain characteristics and of other issues such as the complexity and cost of filters forms the core of the important field of filter design.

§6.5 First-Order and Second-order Continuous-time Systems

§6.5.1 First-order Continuous-time Systems

$$\tau \frac{dy}{dt} + y = x$$

$$X(s) \longrightarrow \boxed{\frac{1}{\tau s+1}} \longrightarrow Y(s)$$

$$\Leftarrow \quad h(t) = \frac{1}{\tau} e^{-t/\tau} u(t)$$

$$s(t) = \int_{-\infty}^{t} h(t-\tau)\, u(\tau)\, d\tau$$

$$= \left[1 - e^{-\frac{t}{\tau}}\right] u(t)$$

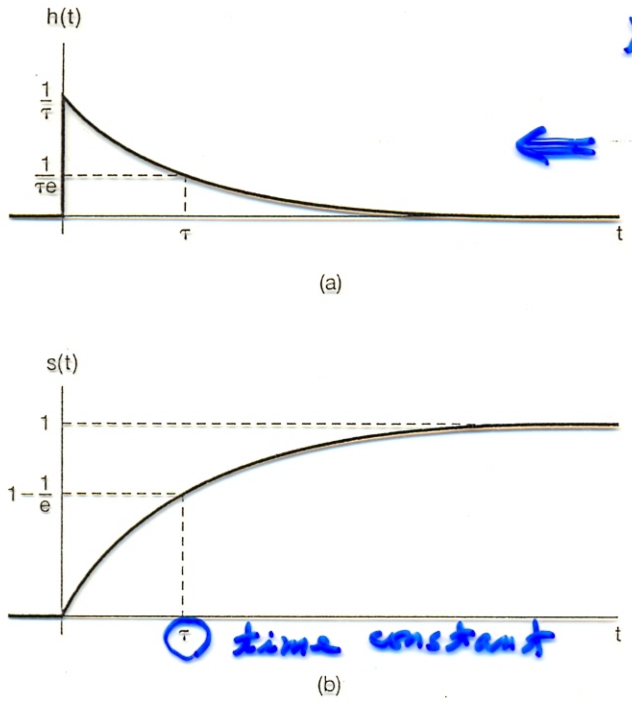

Figure 6.19 Continuous-time first-order system: (a) impulse response; (b) step response.

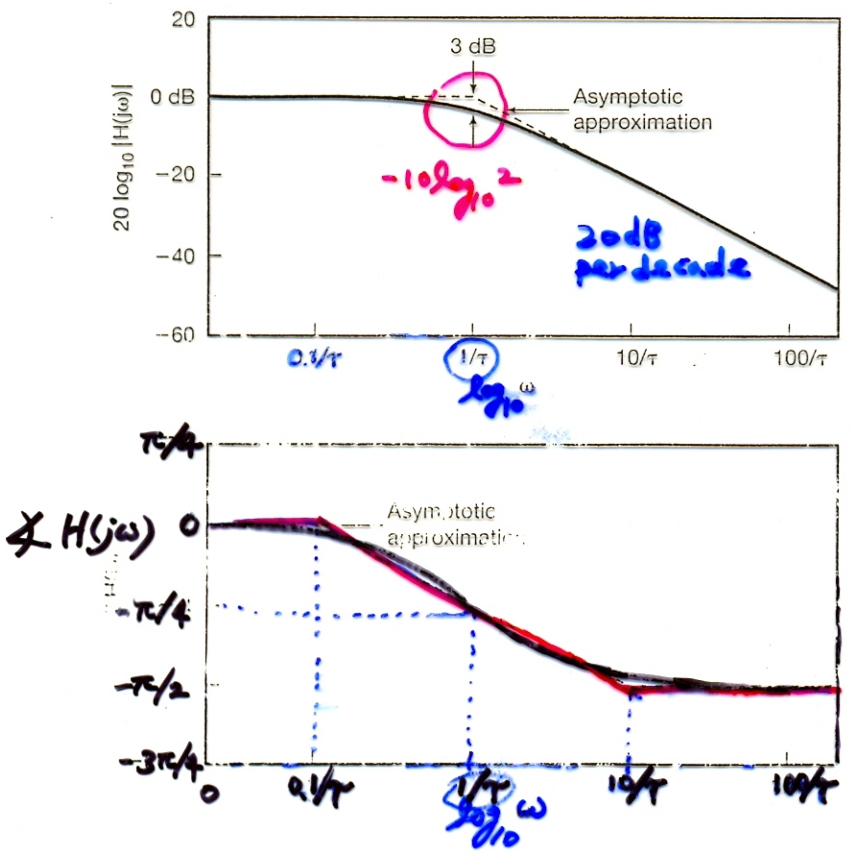

$$20\log_{10}|H(j\omega)| = -10\log_{10}\left[(\omega\tau)^2+1\right]$$

$$\simeq \begin{cases} 0 & \text{for } \omega \ll 1/\tau \\ -20\log_{10}\omega - 20\log_{10}\tau & \text{for } \omega \gg 1/\tau. \end{cases} \quad (6.29)$$

$$\measuredangle H(j\omega) = -\tan^{-1}\omega\tau$$

$$\simeq \begin{cases} 0, & \omega \le 0.1/\tau \\ -(\pi/4)\left[\log_{10}\omega\tau + 1\right], & 0.1/\tau \le \omega \le 10/\tau \\ -(\pi/2), & \omega \ge 10/\tau \end{cases} \quad (6.29)$$

Remarks : $H(s) \triangleq \tau s + 1$

$$20\log_{10}|H(j\omega)| = +10\log_{10}\left[(\omega\tau)^2+1\right]$$

§ 6.5.2 Second-order Continuous-time Systems

$$y''(t) + 2\zeta\omega_n y'(t) + \omega_n^2 y(t) = \omega_n^2 x(t) \quad (6.31)$$

then [except for a scale factor of k on $x(t)$] the equation of motion for the system of Figure 6.21 reduces to eq. (6.31).

The frequency response for the second-order system of eq. (6.31) is

$$H(s) = \frac{\omega_n^2}{s^2 + 2\zeta\omega_n s + \omega_n^2} \Rightarrow H(j\omega) = \frac{\omega_n^2}{(j\omega)^2 + 2\zeta\omega_n(j\omega) + \omega_n^2}. \quad (6.33)$$

The denominator of $H(j\omega)$ can be factored to yield

$$H(j\omega) = \frac{\omega_n^2}{(j\omega - c_1)(j\omega - c_2)},$$

where

$$\begin{aligned} c_1 &= -\zeta\omega_n + \omega_n\sqrt{\zeta^2 - 1}, \\ c_2 &= -\zeta\omega_n - \omega_n\sqrt{\zeta^2 - 1}. \end{aligned} \quad (6.34)$$

For $\zeta \neq 1$, c_1 and c_2 are unequal, and we can perform a partial-fraction expansion of the form

$$H(j\omega) = \frac{M}{j\omega - c_1} - \frac{M}{j\omega - c_2}, \quad (6.35)$$

where

$$M = \frac{\omega_n}{2\sqrt{\zeta^2 - 1}}. \quad (6.36)$$

From eq. (6.35), the corresponding impulse response for the system is overdamped

$$h(t) = M[e^{c_1 t} - e^{c_2 t}]u(t). \quad (\zeta > 1) \quad (6.37)$$

If $\zeta = 1$, then $c_1 = c_2 = -\omega_n$, and

$$H(j\omega) = \frac{\omega_n^2}{(j\omega + \omega_n)^2}. \quad (6.38)$$

From Table 4.2, we find that in this case the impulse response is critically damped

$$h(t) = \omega_n^2 t e^{-\omega_n t} u(t). \quad (\zeta = 1) \quad (6.39)$$

Note from eqs. (6.37) and (6.39), that $h(t)/\omega_n$ is a function of $\omega_n t$. Furthermore, eq. (6.33) can be rewritten as

$$h(t) \triangleq \omega_n \hat{h}(\omega_n t) \xleftrightarrow{\mathcal{F}} H(j\omega) = \frac{1}{(j\omega/\omega_n)^2 + 2\zeta(j\omega/\omega_n) + 1},$$

from which we see that the frequency response is a function of ω/ω_n. Thus, changing ω_n is essentially identical to a time and frequency scaling.

The parameter ζ is referred to as the *damping ratio* and the parameter ω_n as the *undamped natural frequency*. The motivation for this terminology becomes clear when

<u>Remark</u>

$$\hat{h}(t) \xleftrightarrow{\mathcal{F}} \frac{1}{(j\omega)^2 + 2\zeta(j\omega) + 1} \quad \text{and} \quad x(at) \xleftrightarrow{\mathcal{F}} X(j\omega/a)/|a|$$

we take a more detailed look at the impulse response and the step response of a second-order system. First, from eq. (6.35), we see that for $0 < \zeta < 1$, c_1 and c_2 are complex, and we can rewrite the impulse response in eq. (6.37) in the form

under damped. $(0<\zeta<1)$

$c_1 = -\zeta\omega_n + j\omega_n\sqrt{1-\zeta^2}$
$c_2 = -\zeta\omega_n - j\omega_n\sqrt{1-\zeta^2}$
$M = \omega_n / 2j\sqrt{1-\zeta^2}$

$$\begin{aligned} h(t) &= \frac{\omega_n e^{-\zeta\omega_n t}}{2j\sqrt{1-\zeta^2}}\{\exp[j(\omega_n\sqrt{1-\zeta^2})t] - \exp[-j(\omega_n\sqrt{1-\zeta^2})t]\}u(t) \\ &= \frac{\omega_n e^{-\zeta\omega_n t}}{\sqrt{1-\zeta^2}}[\sin(\omega_n\sqrt{1-\zeta^2})t]u(t). \end{aligned} \tag{6.40}$$

Thus, for $0 < \zeta < 1$, the second-order system has an impulse response that has damped oscillatory behavior, and in this case the system is referred to as being *under-damped*. If $\zeta > 1$, both c_1 and c_2 are real and negative, and the impulse response is the difference between two decaying exponentials. In this case, the system is *overdamped*. The case of $\zeta = 1$, when $c_1 = c_2$, is called the *critically damped* case. The impulse responses (multiplied by $1/\omega_n$) for second-order systems with different values of ζ are plotted in Figure 6.22(a).

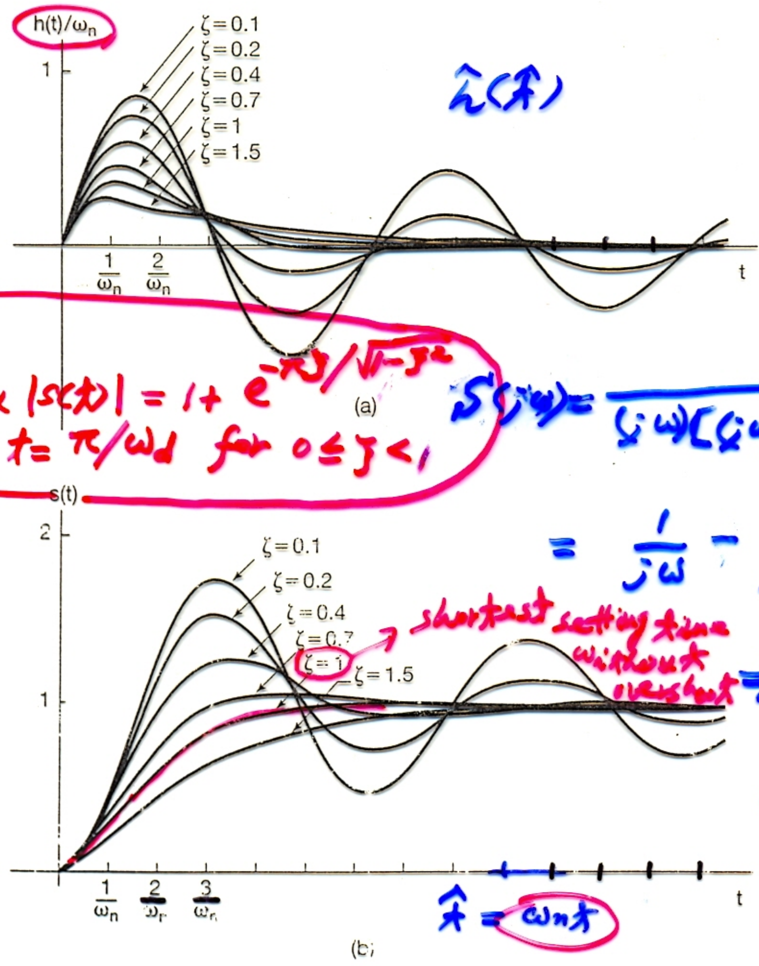

$\hat{h}(\hat{t})$

$\hat{t} = \omega_n t$

max $|s(t)| = 1 + e^{-\pi\zeta/\sqrt{1-\zeta^2}}$ at $t = \pi/\omega_d$ for $0 \le \zeta < 1$

$\zeta = 1$: shortest settling time without overshoot

$$S(j\omega) = \frac{\omega_n^2}{(j\omega)[(j\omega)^2 + 2\zeta\omega_n(j\omega) + \omega_n^2]} = \frac{1}{j\omega} - \frac{(\zeta\omega_n/\omega_d + j)/2}{j\omega + \zeta\omega_n - j\omega_d} - \frac{(\zeta\omega_n/\omega_d - j)/2}{j\omega + \zeta\omega_n + j\omega_d}$$

$$\Rightarrow s(t) = 1 - e^{-\zeta\omega_n t}\left[\frac{\zeta\omega_n}{\omega_d}\sin\omega_d t + \cos\omega_d t\right],$$

where $\omega_d \triangleq \omega_n\sqrt{1-\zeta^2}$: natural freq.

Figure 6.22 Response of continuous-time second-order systems with different values of the damping ratio ζ: (a) impulse response; (b) step response.

Remark

The ringing frequency is usually the natural frequency of the dominant pole. □

$$20\log_{10}|H(j\omega)| = -10\log_{10}\left\{\left[1-\left(\frac{\omega}{\omega_n}\right)^2\right]^2 + 4\zeta^2\left(\frac{\omega}{\omega_n}\right)^2\right\} \quad (6.43)$$

$$\simeq \begin{cases} 0, & \text{for } \omega \ll \omega_n \\ -40\log_{10}\omega + 40\log_{10}\omega_n, & \text{for } \omega \gg \omega_n \end{cases} \quad (6.44)$$

$\max |H(j\omega)| = 1/2\zeta\sqrt{1-\zeta^2}$ for $0<\zeta<1/\sqrt{2}$

at $\omega_{max} = \omega_n\sqrt{1-2\zeta^2}$

$\nexists$ overshoot if $\zeta \geq 1/\sqrt{2}$

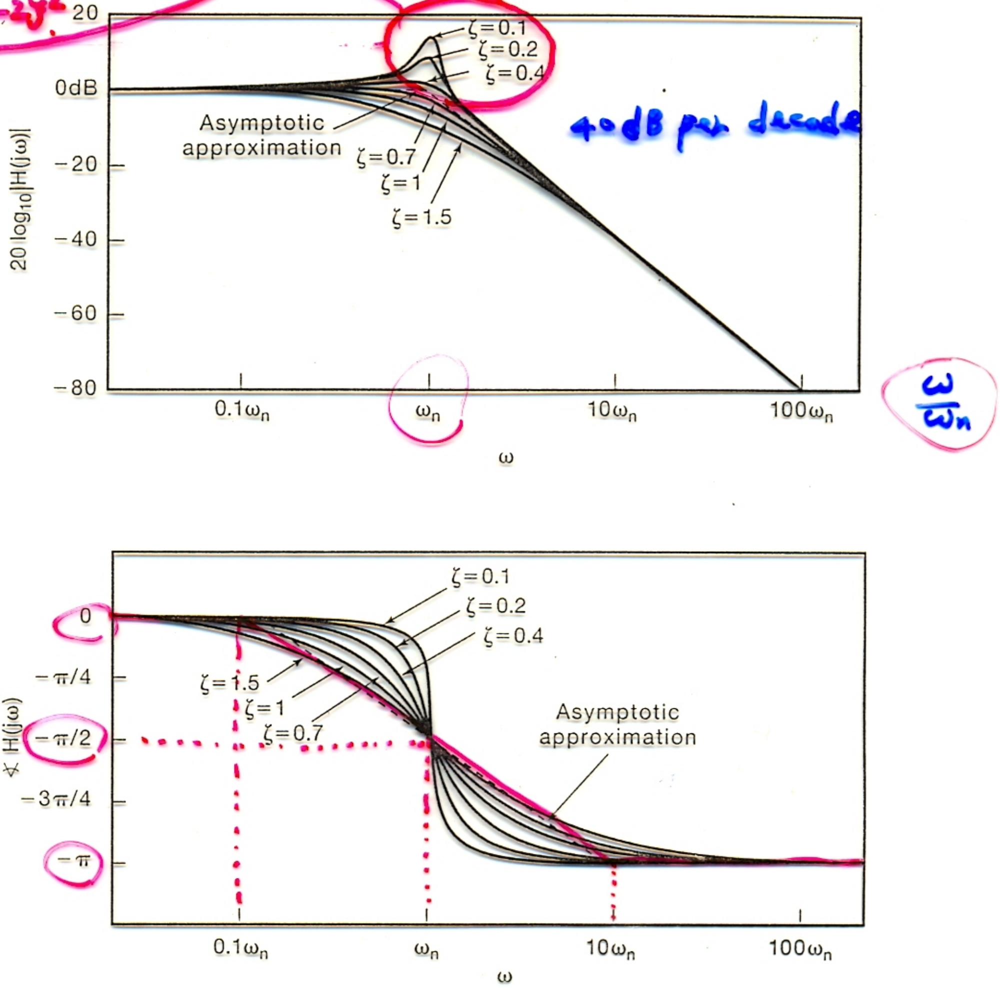

Figure 6.23 Bode plots for second-order systems with several different values of damping ratio ζ.

Therefore, the low-frequency asymptote of the log magnitude is the 0-dB line, while the high-frequency asymptote [given by eq. (6.44)] has a slope of −40 dB per decade; i.e., $|H(j\omega)|$ decreases by 40 dB for every increase in ω of a factor of 10. Also, note that the two straight-line asymptotes meet at the point $\omega = \omega_n$. Thus, we obtain a straight-line approximation to the log magnitude by using the approximation given in eq. (6.44) for $\omega \leq \omega_n$. For this reason, ω_n is referred to as the break frequency of the second-order system. This approximation is also plotted (as a dashed line) in Figure 6.23.

We can, in addition, obtain a straight-line approximation to $\sphericalangle H(j\omega)$, whose exact expression can be obtained from eq. (6.33):

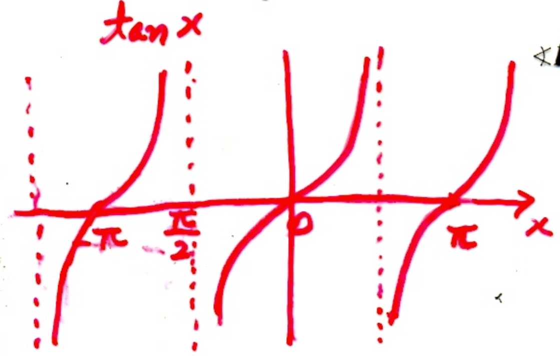

$$\sphericalangle H(j\omega) = -\tan^{-1}\left(\frac{2\zeta(\omega/\omega_n)}{1-(\omega/\omega_n)^2}\right) \quad (6.45)$$

$\zeta \geq 1$

$$\simeq \begin{cases} 0, & \omega \leq 0.1\,\omega_n \\ -\frac{\pi}{2}\left[\log_{10}\frac{\omega}{\omega_n} + 1\right], & 0.1\,\omega_n \leq \omega \leq 10\,\omega_n \\ -\pi, & \omega \geq 10\,\omega_n \end{cases}$$

<Example 6.5>

$$H(j\omega) = \frac{100(1+j\omega)}{(10+j\omega)(100+j\omega)} = \left(\frac{1}{10}\right)\left(\frac{1}{1+j\omega/10}\right)\left(\frac{1}{1+j\omega/100}\right)(1+j\omega)$$

$$= \left(\frac{1}{10}\right)(1+j\omega)\left(\frac{1}{1+j\omega/10}\right)\left(\frac{1}{1+j\omega/100}\right)$$

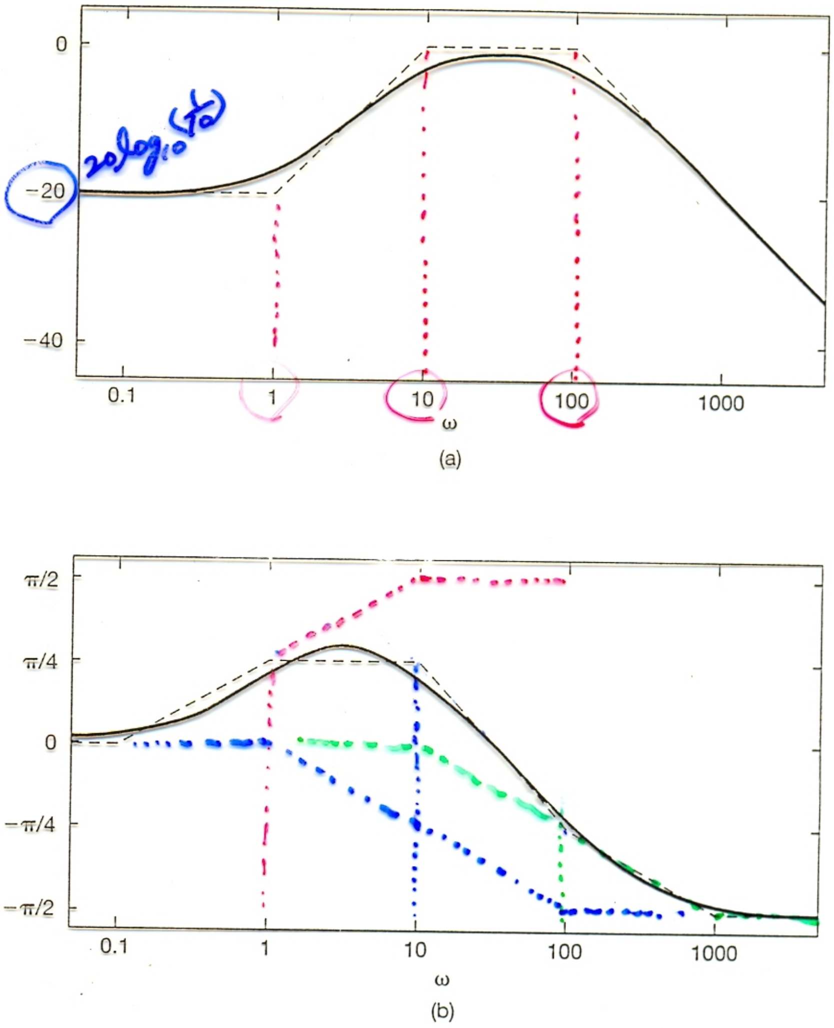

Figure 6.25 Bode plot for system function in Example 6.5: (a) magnitude; (b) phase.

<Example 6.5>′

$$H(j\omega) = \frac{K}{j\omega} \Rightarrow$$

$$\Rightarrow \begin{cases} 20\log_{10}|H(j\omega)| = 20\log_{10}|K| - 20\log_{10}\omega & \text{for } \omega > 0 \\ \measuredangle H(j\omega) = \begin{cases} -\pi/2 & \text{if } K>0 \\ +\frac{\pi}{2} & \text{if } K<0 \end{cases} \end{cases}$$